Automated SQUID tuning procedure for kilo-pixel arrays of TES bolometers on the Atacama Cosmology Telescope

E.S. Battistelli[a,b], M. Amiri[a], B. Burger[a], M.J. Devlin[c], S.R. Dicker[c], W.B. Doriese[d], R. Dünner[e], R.P. Fisher[f], J.W. Fowler[f], M. Halpern[a], M. Hasselfield[a], G.C. Hilton[d], A.D. Hincks[f], K.D. Irwin[d], M. Kaul[c], J. Klein[c], S. Knotek[a], J.M. Lau[g], M. Limon[h], T.A. Marriage[i], M.D. Niemack[f], L. Page[f], C.D. Reintsema[d], S.T. Staggs[f], D.S. Swetz[c], E.R. Switzer[f], R.J.Thornton[c], and Y. Zhao[f]

[a]Dept. of Physics and Astronomy, University of British Columbia, Vancouver, BC, V6T 1Z1, Canada;
[b]Dept. of Physics, University of Rome "La Sapienza", Piazzale Aldo Moro 5, I-00185, Rome, Italy;
[c]Dept. of Physics and Astronomy, University of Pennsylvania, 209 South 33rd Street, Philadelphia, PA 19104, USA;
[d]National Institute of Standards and Technology, 325 Broadway, Boulder, CO 80305, USA;
[e]Dept. de Astronomía y Astrofísica, Facultad de Física, Pontificia Universidad Católica de Chile, Casilla 306, Santiago 22, Chile;
[f]Dept. of Physics, Jadwin Hall, Princeton University, Princeton, NJ 08544-0708, USA;
[g]Dept. of Physics, Stanford University, 382 Via Pueblo Mall, Stanford, CA 94305, USA;
[h]Columbia Astrophysics Laboratory, 550 W. 120th St. Mail Code 5247, New York, NY 10027, USA;
[i]Dept. of Astrophysical Sciences, Peyton Hall, Princeton University, Princeton, NJ 08544, USA.

ABSTRACT

The Atacama Cosmology Telescope observes the Cosmic Microwave Background with arcminute resolution from the Atacama desert in Chile. For the first observing season one array of 32 x 32 Transition Edge Sensor (TES) bolometers was installed in the primary ACT receiver, the Millimeter Bolometer Array Camera (MBAC). In the next season, three independent arrays working at 145, 220 and 280 GHz will be installed in MBAC. The three bolometer arrays are each coupled to a time-domain multiplexer developed at the National Institute of Standard and Technology, Boulder, which comprises three stages of superconducting quantum interference devices (SQUIDs). The arrays and multiplexers are read-out and controlled by the Multi Channel Electronics (MCE) developed at the University of British Columbia, Vancouver.

A number of experiments plan to use the MCE as read-out electronics and thus the procedure for tuning the three stage SQUID system is of general interest. Here we describe the automated array tuning procedures and algorithms we have developed. During array tuning, the SQUIDs are biased near their critical currents. SQUID feedback currents and lock points are selected to maximize linearity, dynamic range, and gain of the SQUID response curves. Our automatic array characterization optimizes the tuning of all three stages of SQUIDs by selecting over 1100 parameters per array during the first observing season and over 2100 parameters during the second observing season. We discuss the timing, performance, and reliability of this array tuning procedure as well as planned and recently implemented improvements.

Keywords: CMB observations, mm and sub-mm arrays, TES bolometers, SQUIDs, Multi-Channel Electronics, array tuning

Send correspondence to E.S. Battistelli
E.S. Battistelli: E-mail: elia@phas.ubc.ca

1. INTRODUCTION

The development of new millimeter and sub-millimeter cameras based on Transition Edge Sensor (TES) bolometer arrays is giving a strong impulse to mm and sub-mm astronomy. These cameras enable high precision Cosmic Microwave Background (CMB) measurements and accurate characterization of sub-mm galaxies, resulting in great progress in Cosmology.

Measurements of the CMB temperature power spectrum at multipoles up to $l \sim 3500$ will enable further characterization of the scalar power law index n_s of the primordial perturbations or identification of deviations from a pure power law.[1] Interactions of the CMB photons with the relativistic plasma in clusters of galaxies and diffuse matter leaves an imprint in the CMB power spectrum at high multipoles and is detectable through the spectral distortion caused by inverse Compton scattering known as the Sunyaev Zel'dovich (SZ) effect.[2] High sensitivity, high angular resolution, and high mapping speed are necessary to perform these observations.

One way to improve the sensitivity of a pixel array when the detectors are photon noise limited is to increase the number of detectors. Multiplexing techniques reduce the number of wires reaching the cold stage of a cryostat housing the detectors and effectively enable a large increase of the number of pixels in mm and sub-mm cameras. Two kinds of SQUID multiplexing techniques have been developed: frequency domain multiplexing (FDM)[3] and time domain multiplexing (TDM).[4] We will focus on the TDM technique developed at NIST. The multiplexing is accomplished by coupling the TESs to superconducting quantum interference device (SQUID) amplifiers which enable high-bandwidth and low-noise read-out.

Accurate choice of the many parameters for the TESs and the SQUIDs of an array is critical for improving sensitivity and minimizing systematics during observations. In this paper we describe, the automated array tuning procedures and algorithms developed for use with the Atacama Cosmology Telescope receiver. We discuss the timing, performance, and reliability of the tuning procedure as well as recently implemented improvements. In Section 2 we briefly describe the Atacama Cosmology Telescope, in Section 3 we present the SQUID tuning algorithms, in Section 4 we describe the TES biasing procedure, and in Section 5 we present the tuning procedures during observations in the first and second observing seasons. This is one of a series of papers[5–9] in these proceedings which describe technical aspects of ACT; the telescope,the cryogenic camera, the control software, the optical characterization, the detectors, and the tuning of the arrays.

2. ATACAMA COSMOLOGY TELESCOPE

The Atacama Cosmology Telescope is an aplanatic 6-meter off-axis Gregorian telescope built for use at millimeter wavelengths.[10] It is located on Cerro Toco at 5190m in the Chilean Andes. The telescope was built by Empire Dynamic Structures Ltd. in Port Coquitlam, BC, Canada* with the motion system provided by KUKA Robotics†.[5] A fixed ground screen and a comoving groundscreen ensure low ground pickup.

ACT aims to measure more than 200 square degrees on the sky to a few μK per $2' \times 2'$ pixel. Observations are made by scanning the entire telescope at constant elevation, 5° peak-to-peak in azimuth every 11 seconds, allowing removal of atmospheric effects and combat of 1/f pickup. ACT regularly slews east and west of the south celestial pole. This results in a cross linked scan pattern, which is important for making high quality maps on degree angular scales.

The Millimeter Bolometer Array Camera (MBAC) is the dedicated camera for ACT.[6,8] It houses three 32×32 arrays of TES, developed at NASA's Goddard Space Flight Center (GSFC), subtending $\approx 22'$ of field of view on the sky.[9,11,12] The three arrays observe the sky through three different spectral bands centered at 145, 220 and 280 GHz. The bands are optimized for efficient observation of the CMB primary anisotropies, for a careful study of the SZ effect, to disentangle foreground emissions from the astrophysical signal of interest, and to match atmospheric transmission at mm wavelengths. In the 2007 season only the 145 GHz array was fielded.

The bolometers' signals are measured through a 3-SQUID-stage TDM system developed at NIST, Boulder. Each bolometer is inductively coupled to a first stage SQUID (SQ1). Every column of the multiplexer comprises

*http://www.amecds.com/

†http://www.kuka.com/

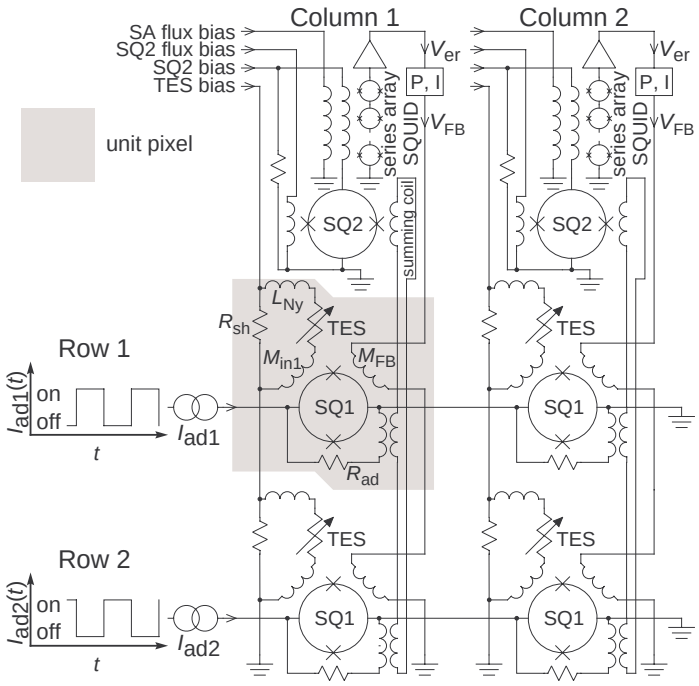

Figure 1. Schematic of a 2-row × 2-column SQUID TDM. Each TES is inductively coupled (M_{in1}) to its own SQ1. An inductive summing coil carries the output signals from all SQ1s in a column to a common SQ2. Rows of SQ1s are sequentially addressed, using I_{ad}, so the signal from one TES at a time per column is passed to that column's SQ2. Finally, the output of each SQ2 is routed to a SA amplifier and then to room-temperature electronics (MCE). In order to keep the nonlinear three-stage SQUID amplifier in a small, linear range, the multiplexer is run as a FLL. The SA output, or error signal (V_{er}), is digitally sampled by the MCE, and then a feedback signal (V_{FB}) is applied inductively to the SQ1 to servo V_{er} to a constant value. In ACT, each kilopixel array is read-out with a 33-row × 32-column TDM.

33 SQ1s (32 coupled to a TES plus 1 dark SQ1) coupled to one single second stage SQUID (SQ2) whose signal is then amplified by a high gain SQUID Series Array (SA). The first two stages are operated at 300 mK, while the SA is near 4 K. Each SQUID has two magnetic inputs, one coming either from the TES or from the previous SQUID stage, and a second one coming from a feedback coil. Because of the intrinsic non-linearity of the SQUID's response, a flux lock loop (FLL) is used to calculate the correct flux to be sent to the SQ1 feedback to compensate for changes in detector current and to keep the amplification chain in a linear regime. A dedicated set of Multi Channel Electronics (MCE)[13] built at the University of British Columbia (UBC), Vancouver, initially developed for the SCUBA2 experiment,[14] is used to supply the detector bias, control the multiplexer and the SQUID amplifiers as well as to read the signals from the 33×32 element arrays. Three independent MCE boxes are used to control the three ACT arrays. Figure 1 shows a schematic of the SQUID TDM developed at NIST.

3. SQUID TUNING

During the array setup, each SQUID is characterized by sweeping the associated feedback current across its full range. The magnetic flux through the SQUID is proportional to the current, and the voltage across the SQUID as a function of the magnetic flux (V(ϕ)) is a periodic sine-like curve. The SQUIDs typically have to be biased at or above their critical current, I_C^{max}, for which the maximum V-ϕ amplitude is achieved, and the feedback currents are chosen in such a way that a SQUID has the highest possible linearity and gain of its response on the V-ϕ curve. Figure 2 shows a current versus voltage characteristic of a SQUID (left) and a SQUID voltage response to a magnetic input for different biases (right). Our automatic array characterization starts by initializing the MCE, the TESs, and the SQUIDs, proceeds with the characterization of the SA followed by the SQ2 and SQ1 stage characterization. Finally, the lock points and the FLL parameters are

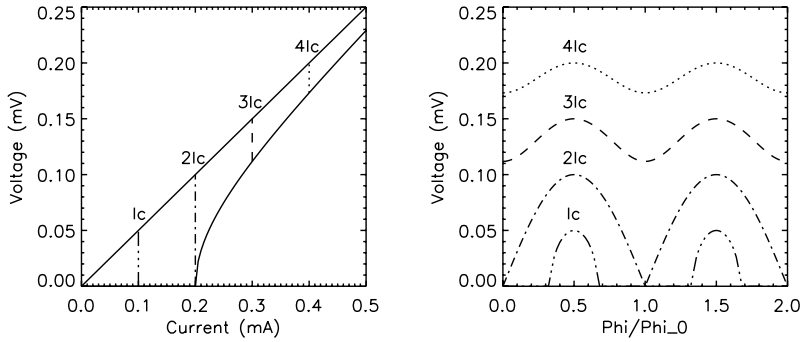

Figure 2. Left: Voltage versus current for a SQUID. The top and bottom lines indicate the limits of the SQUID response. A change of one flux quanta inside the SQUID loop results in an oscillation between the two limits as shown for the constant bias currents I_c, 2 I_c, 3 I_c, and 4 I_c by the dotted and dashed lines. The I_c indicated here is the critical current of the two Josephson junctions that form the SQUID. Right: The SQUID voltage response as a function of the applied magnetic flux (V-ϕ curve) for the aforementioned bias currents. The maximum V-ϕ amplitude is achieved at a bias current of I = 2 I_c = I_C^{max}. Above this value, the V-ϕ curves appear more sinusoidal, but have a smaller peak-to-peak amplitude.

asserted, and confirmed to keep each pixel "locked." The original array autotuning program developed for ACT does a complete setup of a 33×32-element array in $\sim$ 4 minutes.

3.1 TES, SQUID, and MCE initialization

The autotuning procedure starts by checking that the communication bit between the Data Acquisition Computer and the MCE is active, and that the system is healthy and ready to start the SQUIDs tuning. The FLL is turned off and the MCE is programmed to read the SA voltage output (i.e. error signal).

A shell script checks whether the SA and SQ2 have nonzero bias[‡]. If the SA and SQ2 biases are off, the program turns them on and waits 3.5 min for thermalization of the 4K stage. The SA I_c^{max} change slightly as the 4 K stage thermalizes, so this procedure is necessary to prevent drifting of the lock points.

In order to perform the autotuning procedure in a magnetic environment similar to the observation environment, the detectors are "biased on". TESs are first biased normal (driving $\sim$4 mA through them) and then are set to the planned bias points ($\sim$0.4 mA). A precise TES bias is calculated after the SQUID tuning using the results of a load curve measurement (see Section 4 for details).

3.2 SQUIDs Series Array characterization: setting the lock points on column basis

Since the SA is the last stage of amplification before the room temperature electronics, it is characterized at the beginning of the tuning procedure. In order to characterize the SA stage, the SQUIDs V-ϕ curves are collected for different SA bias currents to select the optimal SA bias (*SA_bias*), which corresponds to the maximum peak-to-peak voltage for each SA response (I_C^{max}). Also, a locking point offset per SA (*lock_point*) is chosen in such a way to maintain linearity during the successive SQUID tuning stages. The target can be chosen to correspond to the SA feedback where the slope of a V-ϕ curve is the highest, or in the mid-point between a maximum and the following minimum (or *vice versa* depending on the sign of the gain) of the sine-like SQUID V-ϕ curve. We have chosen the second option in order to maximize the input dynamic range rather than to maximize the gain.

We have found that the SA I_C^{max} values are related to the particular SQUIDs and their temperatures[§]. In order to minimize the variability in parameters between different nights of observations, the SA I_C^{max} have been carefully measured for each SA and fed as input parameters to the autotuning program. In addition to

[‡]The biases are turned off for recycling, and are also set to zero after a power outage.

[§]The SA temperature in MBAC will be regulated using a servo system during the second observing season.

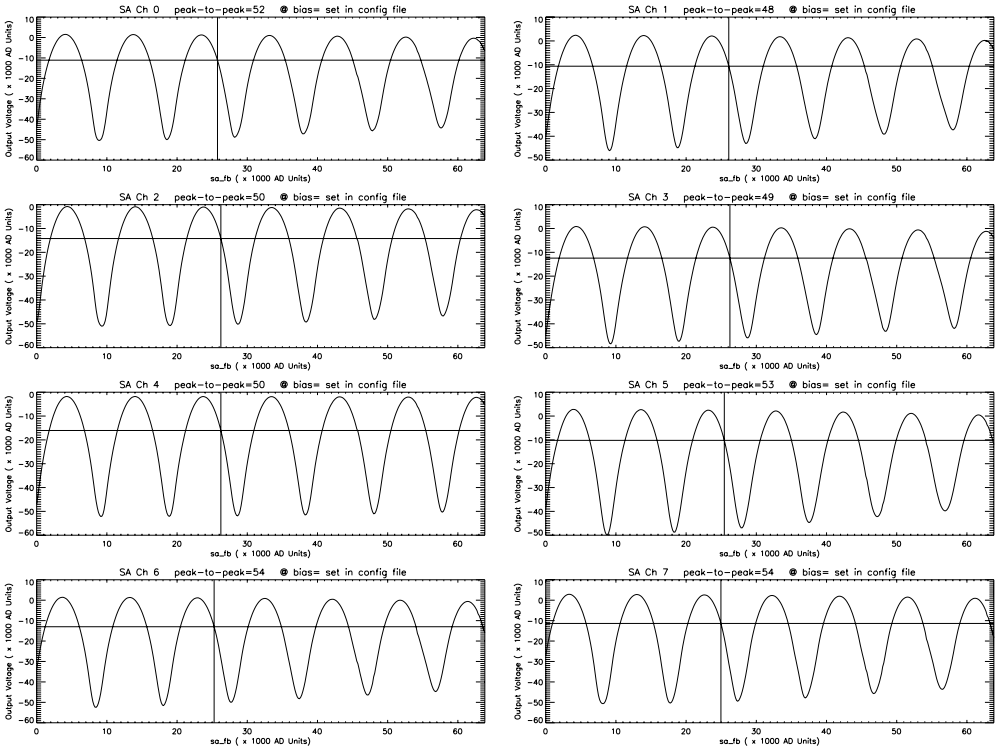

Figure 3. SA V-ϕ curves for columns 0 to 7 of the 145 GHz ACT array. The SA are biased at their I_C^{max}. The x-axis is the feedback current to the SA which is proportional to the magnetic flux through the loop. One period is one quantum magnetic flux. The y-axis is the voltage across the full SA. Four of these plots are produced by the autotuning program for each array. The *lock_point*s, chosen on column basis, are shown in this plot as horizontal lines. They correspond to the SA feedback (vertical lines) that maximizes the input dynamic range. See text for details.

the *SA_bias*, this step allows one to set 32 *lock_point*s, one per array column, which are stored and subsequently used in the autotuning procedure. In Figure 3 the SA V-ϕ curves for columns 0 to 7 of the 145 GHz ACT array together with the selected *lock_point*s are shown.

3.3 Second Stage SQUIDs characterization: setting the SA feedback currents

Coupling of the SQ2 stage to the SA is optimized by an accurate choice of the SA feedback currents. To select the values of these currents, characterization of the SQ2 stage is necessary. The same method applied for the SA cannot, however, be directly applied to the SQ2s. A ramp of the SQ2 feedback current produces an output on the SA which is a composite function of their V-ϕ curves; this makes it difficult to interpret the SQ2 V-ϕ curve independently.

The way we measure the SQ2 V-ϕ curves is by using a closed servo loop procedure. For a given value of the SQ2 bias current, we sweep the SQ2 feedback current from zero to full scale. At each value of the SQ2 feedback current we adjust the SA feedback current to null the effect of the SQ2 and bring the SA output voltage back to the target output voltage chosen above. Calculation of the closed-loop SA feedback current is done in software by a C program which uses a simple proportional feedback term. The resulting curves (SA feedback *vs* SQ2 feedback, shown in Figure 4) are representative of the SQ2 V-ϕ curves and can be used to choose the optimal SQ2 bias (*SQ2_bias*) and SA feedback (*SA_fb*) currents.

During observations, the 32 *SQ2_bias*'s are held fixed to $\sim 1.5 - 2$ times the maximum SQUID critical current. By slightly over-biasing SQ2, we maximize the dynamic impedance (dV/dI) of SQ2, so as to minimize the L/R time constant of the SQ2-output / SA-input loop, effectively increasing the bandwidth. Also, since the SQ2 V-ϕ amplitude is smaller than at I_C^{max}, this reduces the probability of any single SQ2 V-ϕ coupling through the non-linear regime of the SA resulting in a change of the flux quantum to which it is locked. In

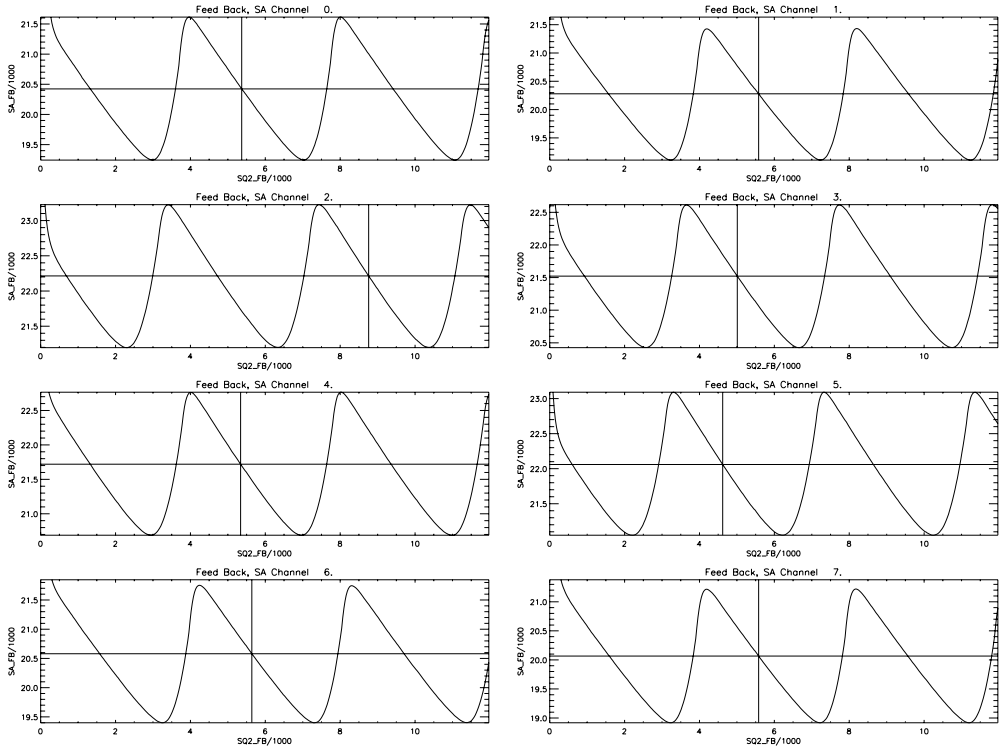

Figure 4. SA feedback *vs* SQ2 feedback curves are representative of the SQ2 V-ϕ curves. Columns 0 to 7 of the 145 GHz ACT array are shown in this Figure. Four of these plots are produced by the autotuning program for each array. This stage allows the selection of the *SA_fb* for each column of the array.

Figure 4 the SQ2 V-ϕ curves for column 0 to 7 of the 145 GHz ACT array together with the selected SA feedback are shown. At the end of this step, 32 *SA_fb* are set and stored by the autotuning program.

3.4 First Stage SQUIDs characterization: setting the SQ2 feedback currents

Similarly to the SQ2-to-SA coupling, the SQ1-to-SQ2 coupling efficiency depends on the choice of the SQ2 feedback currents. In order to select them, the SQ1 stage has to be characterized. An identical closed loop technique is used for the SQ1 stage to choose optimal SQ1 bias and SQ2 feedback currents i.e. (*SQ1_bias* and *SQ2_fb*). In this case, however, one SQ1 bias current (*SQ1_bias*) must be chosen for optimum behavior of the 32 SQ1s of each row. We determine I_C^{max} for each of the 32 SQ1 in a row, and *SQ1_bias* for that row is chosen to be 1.5 times the mean I_C^{max}.

Since we assign one *SQ2_fb* value for each SQ2, the *SQ2_fb* values are also a compromise between the 33 SQ1s of a given column[¶]. Different approaches can be followed in this case to optimize the choice: the most accurate one would involve a measurement of all the optimal *SQ2_fb* for every row and column of the array (i.e. 32×33 values) and the minimization of a χ^2 function to optimize this choice[15] within each column. To limit the length of the calculation, we have chosen to run the closed loop procedure on the SQ1 only on one row. The median optimal *SQ2_fb* within each column was selected as the tuning row for use in this procedure of all future autotuning. This choice of the 32 *SQ2_fb* has the intrinsic problem that slightly different SQ1s of one column couple differently with their SQ2. As we will see in the following, this can result in multi-valued lock-points with different V-ϕ slopes of the same sign because the variability in the SQ1 I_C^{max} values results in roughly proportional variability in the optimal *SQ2_fb* values for the SQ1. Figure 6 shows an example of multi-valued lock-points. In Figure 5 the SQ1 V-ϕ curves for columns 0 to 7, and 8 different rows of the 145

[¶]In preparation for the second observing season we have developed the multiplexing of the *SQ2_fb*. This makes the choice of the *SQ2_fb* accurate for each row of the array. See Section 5.2 for details.

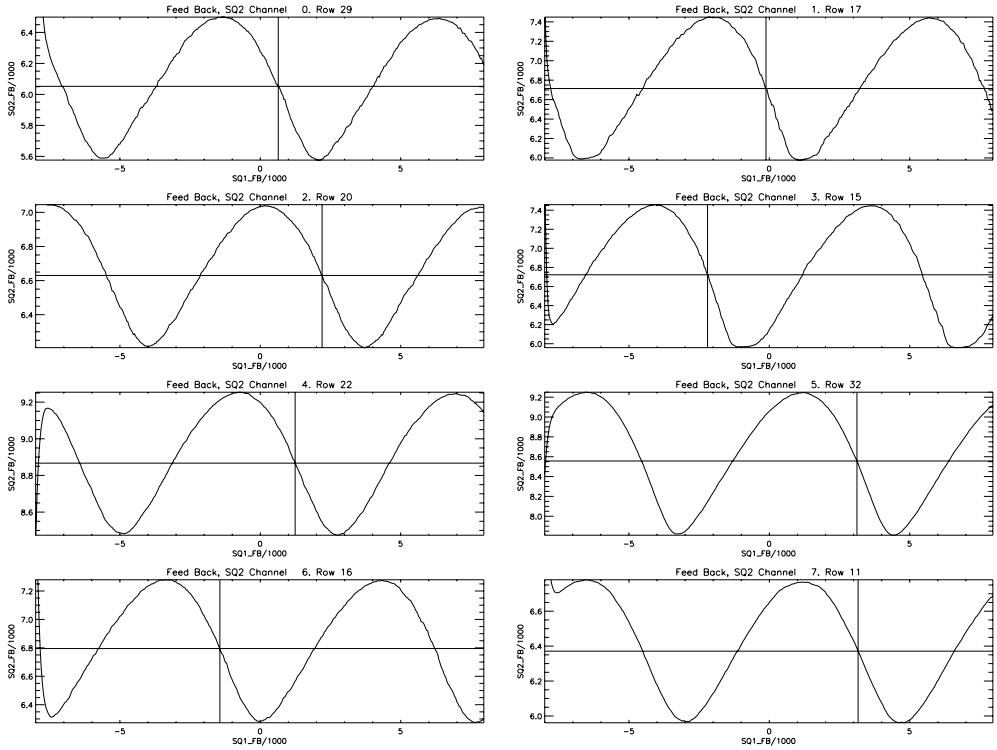

Figure 5. SQ2 feedback *vs* SQ1 feedback curves are representative of the SQ1 V-ϕ curves. Columns 0 to 7 for 8 different rows of the 145 GHz ACT array are shown. Row 29, 17, 20, 15, 22, 32, 16, and 11 have been selected to give the median optimal *SQ2_fb* within each column. This stage allows the selection of the *SQ2_fb*.

GHz ACT array, together with the selected SQ2 feedback, are shown. The 32 *SQ2_fb* are set and stored by the autotuning procedure in this stage.

3.5 Flux Lock Loop: setting the final lock points on pixel basis

The final step of the locking procedure is an open loop acquisition of the SA output from each detector in the array while sweeping the SQ1 feedback. This allows fine tuning of the *lock_point*s for every individual detector. The 1056 *lock_point* values are then set and stored by the autotuning program by centering the curves on zero output. The ramp of the SQ1 feedback is repeated twice, before and after the final *lock_point* choice. The output signal allows one to calculate the gain (and its sign) of the whole SQUID chain for each detector and to check for possible multi-valued lock points. We have observed that typically 2% of the pixels show the multi-valued lock-point feature and other 4% of the pixels, despite being properly locked, risk to show multi-valued lock point feature upon drifts (see Figure 6 for details).

All the previous steps are performed by observing the SA voltage output (error) signal. The firmware-based FLL, effectively a proportional-integral (PI) servo loop, can now be turned on, and the SQ1 feedback necessary to compensate the TES input is digitally calculated and acquired by the MCE for every pixel of the array.

The PI loop parameters have been chosen in order to prevent the PI-servo-loop from acting as low-pass filter (if set too low) or driving the SQ1 feedback into oscillation (if set too high). We have found that we can fully compensate for the changes in detector current using only an integral term (I-term). The selected I-term was chosen to be roughly a factor of two below the value that drove the PI loop into high frequency oscillations.[16]

During data acquisition, the SQ1 feedback signal is read at ∼15 kHz, low-pass filtered and reported at ∼400 Hz by the MCE in 32-bit numbers. At this stage of the autotuning process, a sample of time ordered data is acquired and the 32 bits are shared between 18 bits of feedback signal and 14 bits of error signal.

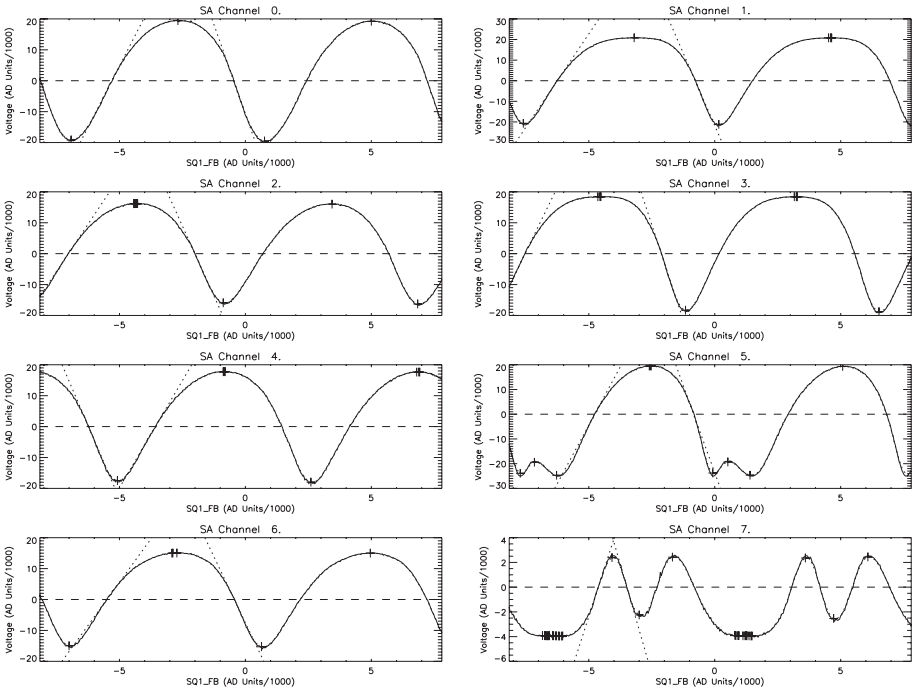

Figure 6. The result of the open loop acquisition for row 32, columns 0 to 7 (i.e. SA channel 0 to 7) of the 145 GHz ACT array is shown here. This represents the full response of the SQUID chain which is acquired (just before turning on the FLL) to calculate the final lock-points, the gain, and to look for those pixel that will show problems while locked. In this example, channel 0, 1, 2, 3, 4, and 6 will lock successfully. Channel 7 has two possible lock points with the same sign and will show multi-valued locking points; channel 5 will lock successfully but the non-perfect choice of the *SQ2_fb* puts it at risk of coming unlocked during data acquisition.

When properly locked, the feedback signal for every pixel should track an incoming signal while the error signal should fluctuate around zero. This is a useful tool for determining whether any particular pixel shows locking problems. We empirically found that if the average of the error signal is larger than twice its standard deviation, then the FLL is not acting efficiently to keep the pixel locked. We typically find that less than 3% of the pixels have locking problems (including the multi-valued locked pixels). For problematic detectors (or those with non-functional SQ1) we have to set the PI parameters to zero. This prevents ramping of the SQ1 feedback line on those detectors, which otherwise couples into the signals of other detectors in the same column.

4. TES TUNING

The TES bolometers are biased on the superconducting transition where their responsivities/dynamic ranges are maximized. ACT uses three different detector bias lines for each 32×32-bolometer array. The detector bias currents are selected at the beginning of each night of observations after the SQUID autotuning process, to maximize the number of detectors on the transition. A load (I-V) curve is acquired on all the bolometers of the array and analyzed to calculate the detector bias current that drives each bolometer to 30% of its normal resistance, R_n (or another predefined percentage of R_n). The median current on each bias line is selected, and the detector bias current is set to that value. After the bias current is known, the detector parameters at that bias are extracted from all the analyzed load curves and stored with subsequently acquired data files for future analysis. This approach often results in as many as 98% of the working detectors of the array being biased between 0.15 and 0.80 R_n, which is considered a good regime for observations.

5. ACT OBSERVATIONS

During observations, the SQUIDs and the TESs have to be tuned each time the magnetic environment changes. The dominant magnetic effects come from the Earth's field, which is modulated by the telescope motion. The desire to minimize the variation of parameters within one night of observations leads to a trade off between frequent array tunings and one single tuning per night of observations.

5.1 First observing season

During the first observing season, given the ACT cross linked observing strategy, we chose to tune SQUIDs and TESs at the beginning of every night of observations, and every time the telescope slewed east-west to account for the change in local magnetic field.

Three different kinds of SQUID tuning procedures have been developed:

- The full autotuning procedure described in Sections 3.1-3.5 is performed at the beginning of the observing night. As mentioned, this procedure sets 32 *SA_fb*, 32 *SQ2_fb*, 1056 *lock_point*s, calculates the gain for every pixel of the array and flags possible poorly locked detectors. It takes about four minutes to perform a full autotuning.
- In the ACT multiplexer, the component most sensitive to external magnetic fields is the summing coil that enables the multiplexing and couples all the SQ1s of one column to their SQ2. We thus expect that the *SQ2_fb* selection would change most when the telescope moves significantly due to the change in the Earth's magnetic field. For this reason, in order to minimize multi-valued and poorly selected lock points we repeated the *SQ2_fb* (Section 3.4) and *lock_point* (Section 3.5) selection every time the telescope changed pointing direction in the sky. It takes about two minutes to perform this short autotuning.
- Despite the difference in the *SQ2_fb* selection, these values already represent a compromise over the 33 rows of each column. For this reason, even if the *SQ2_fb*'s change by a small amount, the overall efficiency is not drastically modified. An even shorter autotuning (type 2) procedure has been set up that only selects *lock_point* values (see Section 3.5). It takes about one minute to perform this short autotuning.

ACT observed from November, 14 2007 to December, 17 2007 with one array of 32x32 TESs observing at 145 GHz. We typically ran a full type 0 autotuning at the beginning of the observing night and three or four type 2 autotuning during observations.

5.2 Second observing season

In 2008 ACT will observe the sky with three TES arrays for the 145, 220 and 280 GHz bands, controlled by three independent MCE boxes and three Data Acquisition Computers. The data acquisition software (i.e. MCE Acquisition Software, MAS) has been modified and many scripts and programs have been optimized for the needs of the ACT observations during the second season. The time elapsed by the full autotuning has been reduced to about two minutes and proportionally for the shorter versions of it. To minimize total cryogenic load, the three arrays are tuned independently, and fast tuning is a premium.

The most significant change for the second season tuning procedure is the ability to multiplex the SQ2 feedback values. This was made possible through hardware and firmware changes in the MCE that allow one to switch the SQ2 feedback currents at the same rate as (and synchronous with) the SQ1 bias. In this way, we have overcame the necessity for a compromise between the 33 rows of one column in the choice of the *SQ2_fb* by selecting the optimal *SQ2_fb* for every row.

The improvement achieved with the multiplexing of the SQ2 feedback currents can be seen by comparing Figure 8 to Figure 7. For each, the final V-ϕ curves for row 11 for columns 0 to 7 are plotted, but the fast SQ2 feedback values are only applied for Figure 8. It is evident that the non-optimal biasing of channels 0 and 3 is improved when the multiplexing is enabled. Also, the peak-to-peak of the displayed curves is in most cases maximized which demonstrates the optimization of the tuning.

In order to take full advantage of this new possibility we plan on running a full, type 0, autotuning at the beginning of the observing night and one short type 1 autotuning after every telescope motion.

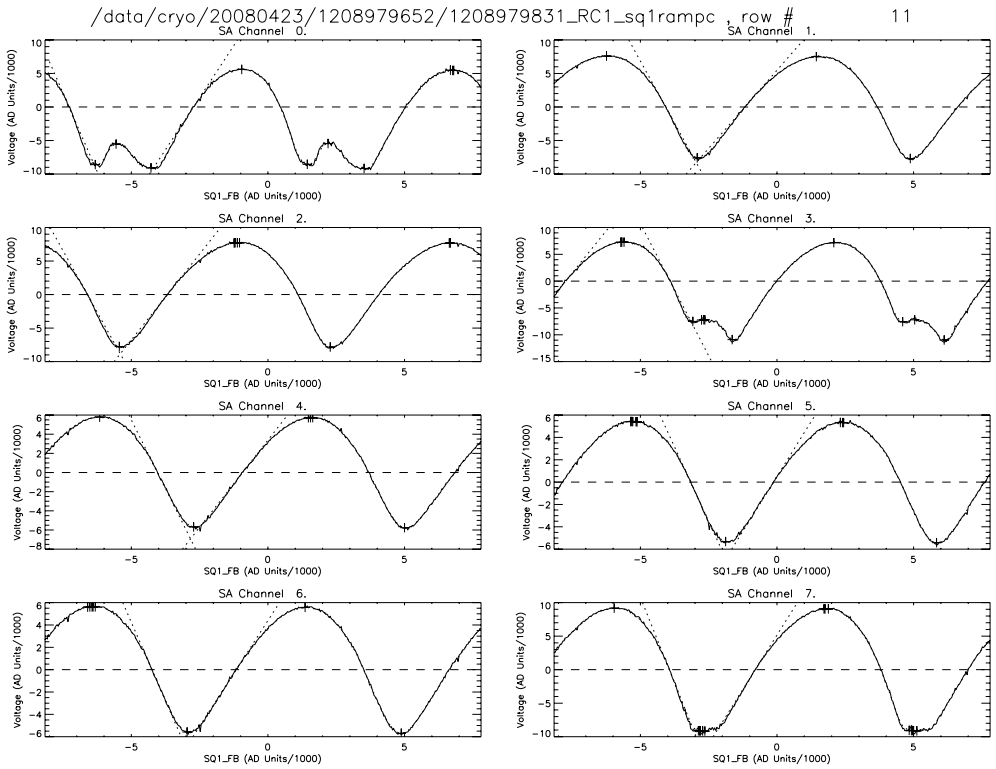

Figure 7. Open loop acquisition of the SA output *vs* the SQ1 feedback after the autotuning procedure has found the feedback and bias currents. Row 11 and column 0 to 7 of the 145 GHz ACT array are shown here. In this acquisition, the SQ2 feedback currents are not multiplexed. Note the extra minima in channel 0 and 3. These are caused by the non perfect choice of the *SQ2_fb* which was optimized for a different row.

6. CONCLUSIONS

The automated SQUID and TES tuning procedure for the ACT camera is presented in this contribution. During the first observing season, the ACT autotuning is executed at the beginning of each observing night and (a short version of it) each time the telescope changes pointing direction. This allows us to select over 1100 bias and feedback currents. During the second observing season, the multiplexing of the SQ2 feedback currents will enable a more accurate tuning performed by selecting over 2100 parameters on the array. All the operations on the MCE in the laboratory or on the ACT site are performed remotely (via the Internet). This effectively increases the manpower spent on the instrument.

ACKNOWLEDGMENTS

This work was supported by the U.S. National Science Foundation through awards AST-0408698 for the ACT project. Funding was also provided by Princeton University and the University of Pennsylvania. The MCE project is funded by the Canadian Foundation for Innovation and its design was developed for the SCUBA2 experiment by the University of British Columbia (Vancouver) and the Astronomy Technology Center (Edinburgh). ESB wishes to thank the Canadian National Science and Engineering Research Council and the Italian Space Agency for supporting his work.

REFERENCES

[1] Kosowsky, A. and Turner, M. S., "CBR anisotropy and the running of the scalar spectral index," *Physical Review D* **52**, 1739–1743 (1995).

[2] Zeldovich, Y. B. and Sunyaev, R. A., "The interaction of matter and radiation in a hot-model universe," *Astrophysics and Space Science* **4**, 301–316 (1969).

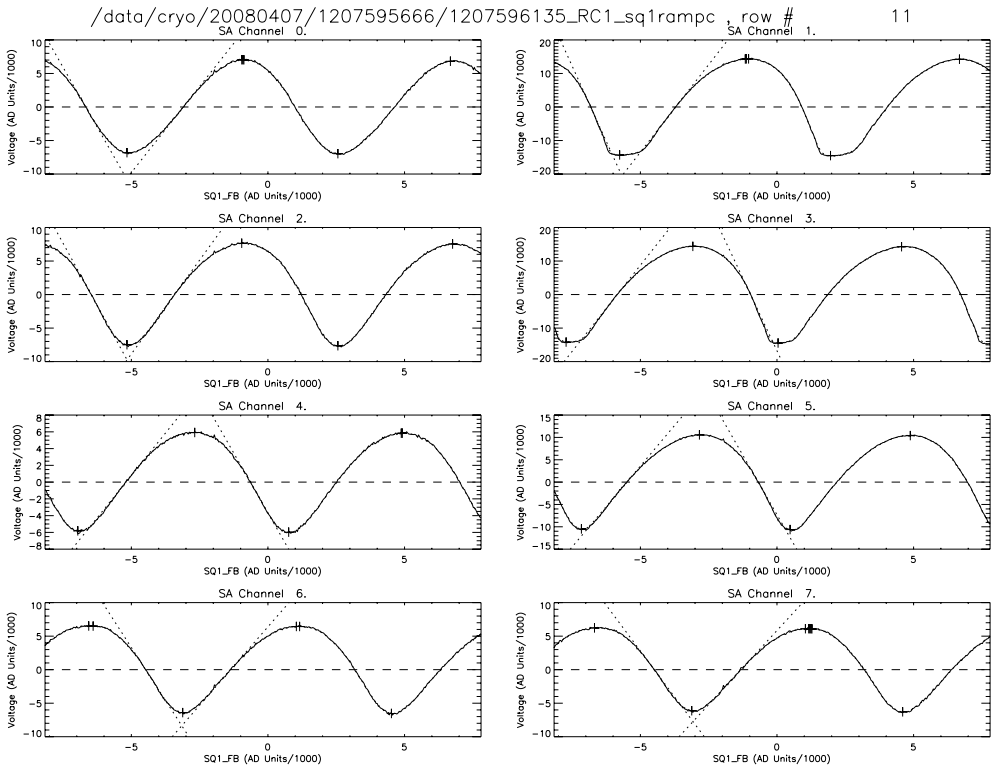

Figure 8. This plots show the same acquisition for the same channels as the previous Figure this time with the SQ2 feedback current multiplexing enabled. The risk of having the multi-valued lock points is eliminated by choosing a proper *SQ2_fb* for each row and by multiplexing their currents synchronously with the *SQ1_bias*.

[3] Yoon, J., Clarke, J., Gildemeister, J. M., Lee, A. T., Myers, M. J., Richards, P. L., and Skidmore, J. T., "Single superconducting quantum interference device multiplexer for arrays of low- temperature sensors," *Applied Physics Letter* **78**, 371 (2001).

[4] Chervenak, J. A., Irwin, K. D., Grossman, E. N., Martinis, J. M., Reintsema, C. D., and Huber, M. E., "Superconducting multiplexer for arrays of Transition Edge Sensors," *Applied Physics Letter* **74**, 4043–4045 (1999).

[5] Hincks, A. D., Ade, P. A. R., Allen, C., Amiri, M., Appel, J. W., Burger, E. S. B. A., Chervenak, J. A., Dahlen, A. J., Denny, S., Devlin, M. J., Dicker, S. R., Doriese, W. B., Dünner, R., Essinger-Hileman, T., Fisher, R. P., Fowler, J. W., Halpern, M., C.Hargrave, P., Hasselfield, M., Hilton, G. C., Irwin, K. D., Jarosik, N., Kaul, M., Klein, J., Lau, J. M., Limon, M., Lupton, R. H., Marriage, T. A., Martocci, K. L., Mauskopf, P., Moseley, S. H., Netterfield, C. B., Niemack, M. D., Nolta, M. R., Page, L., Parker, L. P., Sederberg, A. J., Staggs, S. T., Stryzak, O. R., Swetz, D. S., Switzer, E. R., Thornton, R. J., Tucker, C., Wollack, E. J., and Zhao, Y., "The effects of the mechanical performance and alignment of the Atacama Cosmology Telescope on the sensitivity of microwave observations," *Also in these Proc. SPIE* .

[6] Swetz, D. S., Ade, P. A. R., Allen, C., Amiri, M., Appel, J., Battistelli, E. S., Burger, B., Chervenak, J., Dahlen, A. J., Das, S., Denny, S., Devlin, M. J., Dicker, S. R., Doriese, W. B., D"unner, R., Essinger-Hileman, T., Fisher, R. P., Fowler, J. W., Gao, X., Hajian, A., Halpern, M., Hargrave, P. C., Hasselfield, M., Hilton, G. C., Hincks, A. D., Irwin, K. D., Jarosik, N., Kaul, M., Klein, J., Knotek, S., Lau, J. M., Limon, M., Lupton, R. H., Marriage, T. A., Martocci, K. L., Mauskopf, P., Moseley, S. H., Netterfield, C. B., Niemack, M. D., Nolta, M. R., Page, L., Parker, L. P., Reid, B. A., Reintsema, C. D., Sederberg, A., Sehgal, N., Sievers, J. L., Spergel, D. N., Staggs, S. T., Stryzak, O. R., Switzer, E. R., Thornton, R. J., Tucker, C., Wollack, E. J., and Zhao, Y., "Instrument design and characterization of the Millimeter Bolometer Array Camera on the Atacama Cosmology Telescope," *Also in these Proc. SPIE* .

[7] Switzer, E. R., Allen, C., Amiri, M., Appel, J., Battistelli, E. S., Burger, B., Chervenak, J., Dahlen, A., Das, S., Devlin, M. J., Dicker, S. R., Doriese, W. B., Dünner, R., Essinger-Hileman, T., Fisher, R. P.,

Gao, J. W. F. X., Halpern, M., Hasselfield, M., Hilton, G. C., Hincks, A. D., Irwin, K. D., Jarosik, N., Kaul, M., Knotek, S., Klein, J., Lau, J. M., Limon, M., Lupton, R., Marriage, T. A., Martocci, K., Moseley, H., Netterfield, B., Niemack, M. D., Nolta, M., Page, L., Parker, L., Reid, B., Reintsema, C. D., Sederberg, A., Sievers, J., Spergel, D., Staggs, S. T., Stryzak, O., Swetz, D. S., Thornton, R., Wollack, E., and Zhao, Y., "Systems and control software for the atacama cosmology telescope," *Also in these Proc. SPIE* .

[8] Thornton, R. J., Ade, P. A. R., Allen, C., Amiri, M., Appel, J., Battistelli, E. S., Burger, B., Chervenak, J., Devlin, M. J., Dicker, S. R., Doriese, W. B., Essinger-Hileman, T., Fisher, R. P., Fowler, J. W., Halpern, M., Hargrave, P. C., Hasselfield, M., Hilton, G. C., Hincks, A. D., Irwin, K. D., Jarosik, N., Kaul, M., Klein, J., Lau, J. M., Limon, M., Marriage, T. A., Martocci, K., Mauskopf, P., Moseley, H., Niemack, M. D., Page, L., Parker, L. P., Reidel, J., Reintsema, C. D., Staggs, S. T., Stryzak, O. R., Swetz, D. S., Switzer, E. R., Tucker, C., Wollack, E. J., and Zhao, Y., "Optomechanical design and performance of a compact three-frequency camera for the MBAC receiver on the Atacama Cosmology Telescope," *Also in these Proc. SPIE* .

[9] Zhao, Y., Allen, C., Amiri, M., Appel, J., Battistelli, E. S., Burger, B., Chervenak, J., Dahlen, A., Denny, S., Devlin, M. J., Dicker, S. R., Doriese, W. B., Dünner, R., Essinger-Hileman, T., Fisher, R. P., Fowler, J. W., Halpern, M., Hilton, G. C., Hincks, A. D., Irwin, K. D., Jarosik, N., Klein, J., Lau, J. M., Marriage, T. A., Martocci, K., Moseley, H., Niemack, M. D., Page, L., Parker, L., Sederberg, A., Staggs, S. T., Stryzak, O. R., Swetz, D. S., Switzer, E. R., Thornton, R. J., and Wollack, E. J., "Characterization of transition edge sensors for the Millimeter Bolometer Array Camera on the Atacama Cosmology Telescope," *Also in these Proc. SPIE* .

[10] Fowler, J. W., Niemack, M. D., Dicker, S. R., Aboobaker, A. M., Ade, P. A. R., Battistelli, E. S., Devlin, M. J., Fisher, R. P., Halpern, M., Hargrave, P. C., Hincks, A. D., Kaul, M., Klein, J., Lau, J. M., Limon, M., Marriage, T. A., Mauskopf, P. D., Page, L., Staggs, S. T., Swetz, D. S., Switzer, E. R., Thornton, R. J., and Tucker, C. E., "Optical design of the Atacama Cosmology Telescope and the Millimeter Bolometric Array Camera," *Applied Optics* **46**, 3444–3454 (2007).

[11] Niemack, M. D. for the ACT collaboration, "Measuring two-millimeter radiation with a prototype multiplexed TES receiver for ACT," *Millimeter and Submillimeter Detectors and Instrumentation for Astronomy III. Edited by Zmuidzinas, Jonas; Holland, Wayne S.; Withington, Stafford; Duncan, William D.. Proceedings of the SPIE* **6275**, 62750C (2006).

[12] Niemack, M. D., Zhao, Y., Wollack, E., Thornton, R., Switzer, E. R., Swetz, D. S., Staggs, S. T., Page, L., Stryzak, O., Moseley, H., Marriage, T. A., Limon, M., Lau, J. M., Klein, J., Kaul, M., Jarosik, N., Irwin, K. D., Hincks, A. D., Hilton, G. C., Halpern, M., Fowler, J. W., Fisher, R. P., Dünner, R., Doriese, W. B., Dicker, S. R., Devlin, M. J., Chervenak, J., Burger, B., Battistelli, E. S., Appel, J., Amiri, M., Allen, C., and Aboobaker, A. M., "A kilopixel array of TES bolometers for ACT: Development, testing, and first light," *J. Low Temp. Phys.* **151**(3-4), 690–696 (2008).

[13] Battistelli, E. S., Amiri, M., Burger, B., Halpern, M., Knotek, S., Ellis, M., Gao, X., Kelly, D., MacIntosh, M., Irwin, K., and Reintsema, C., "Functional description of read-out electronics for time-domain multiplexed bolometers for millimeter and sub-millimeter astronomy," *Journal of Low Temperature Physics* (2008).

[14] Holland, W., MacIntosh, M., Fairley, A., Kelly, D., Montgomery, D., Gostick, D., Atad-Ettedgui, E., Ellis, M., Robson, I., Hollister, M., Woodcraft, A., Ade, P., Walker, I., Irwin, K., Hilton, G., Duncan, W., Reintsema, C., Walton, A., Parkes, W., Dunare, C., Fich, M., J.Kycia, Halpern, M., Scott, D., Gibb, A., Molnar, J., Chapin, E., Bintley, D., Craig, S., Chylek, T., Jenness, T., Economou, F., and Davis, G., "SCUBA-2: a 10,000-pixel submillimeter camera for the James Clerk Maxwell Telescope," *Millimeter and Submillimeter Detectors and Instrumentation for Astronomy III. Edited by Zmuidzinas, Jonas; Holland, Wayne S.; Withington, Stafford; Duncan, William D.. Proceedings of the SPIE* **6275**, 62751E (2006).

[15] Irwin, K. *private communication* .

[16] Niemack, M. D., "Towards dark energy: Design, development, and preliminary data from ACT," *PhD thesis, Princeton University Physics Department* (2008).